

Cathodic Protection Measurement and Modeling

Erik K. Saathoff , *Graduate Student Member, IEEE*, Michael J. Bishop , Isabelle C. Levitsky , Jacob D. Skimmons , Aaron W. Langham , *Graduate Student Member, IEEE*, and Steven B. Leeb , *Fellow, IEEE*

Abstract—Marine structures and ships fight a constant battle against corrosion. Sacrificial anodes and impressed-current cathodic protection (ICCP) are two common protection techniques. Many structures employ a hybrid configuration of both, in the hopes that the combination provides more protection than either does individually. Doing so, however, can create situations in which these techniques interfere with each other. It is essential to verify that protection extends adequately to all areas of the structure. This paper describes instrumentation and measurement strategies to determine the corrosion potential and extent of ICCP protection in difficult-to-reach areas on ships. A case study is presented for these methods on a vessel that experienced severe galvanic corrosion damage in its stern tube. Operators of mission critical marine structures can use these insights to tune and improve corrosion protection schemes before damage manifests.

Index Terms—Corrosion measurement, cathodic protection, nonintrusive instrumentation

I. KEEPING YOUR METAL

Ships and other metallic structures in seawater exist in a harsh and destructive environment. In addition, ship components such as the hull, propellers, and bow thrusters generally consist of dissimilar metals [1]. Without a proactive protection scheme, corrosion is inevitable. Corrosion causes substantial rust and pitting that affects structural integrity and increases drag. Rehabilitation of corroded structures can cost millions of dollars and extend repair periods, as large sections of metal must be replaced. Accordingly, a variety of corrosion prevention techniques have been developed and deployed. Coatings and paints physically block the electrochemical reaction associated with corrosion. However, coatings are imperfect and allow leakage of current and interaction with an electrolyte that leads to corrosion. The coating will fail with time if other protection measures, such as cathodic protection, are not employed. Cathodic protection alters the electrochemistry such that corrosion does not occur in valued components. This paper presents measurement techniques and instrumentation tools for the verification of cathodic protection on seagoing ships.

Corrosion of metals in seawater is fundamentally a reduction-oxidation reaction. In such a reaction one metal “reduces” (i.e., gains electrons) and one metal “oxidizes” (i.e., loses electrons). Inherent to each metal is an affinity

The authors gratefully acknowledge the support of the Office of Naval Research NEPTUNE program. (*Corresponding author: Erik K. Saathoff*)

E. Saathoff, A. Langham, and S. Leeb are with the Department of Electrical Engineering and Computer Science, Massachusetts Institute of Technology, Cambridge, MA 02139, USA (e-mail: saathoff@mit.edu; alangham@mit.edu; sbleeb@mit.edu)

M. Bishop and J. Skimmons are with the United States Coast Guard, Washington, DC 20032, USA.

I. Levitsky is with the United States Coast Guard Academy, New London, CT 06320, USA (e-mail: isabelle.c.levitsky@uscga.edu)

for reducing, as indicated by the standard reduction potential table [2]. Metals with lower reduction potentials preferentially oxidize, and will act as anodes and give up electrons to metals with higher reduction potentials, acting as cathodes. Ion exchange occurs in the electrolyte to maintain charge neutrality. Oxidization of the anodic metal at the electrolyte interface gives rise to corrosion in forms such as rust and dissolution. For a steel-hulled ship with a stainless steel propeller in seawater, the steel acts as the anode. Since the stainless steel is more “noble” (i.e., has a higher reduction potential), it becomes the cathode. In the absence of protection, the steel hull will corrode as it loses electrons. Cathodic protection protects against corrosion by turning less noble metals into cathodes.

Sacrificial anode cathodic protection (SACP) operates by introducing a metal with a lower reduction potential than the other metals to be protected. If the difference in potentials is high enough and the sacrificial anode has sufficient surface area exposed to the electrolyte, then electrons will flow into the other exposed metals, making them cathodic and preventing their oxidization. In saltwater applications, zinc anodes are typically used as the sacrificial anode [3]–[6]. Although this technique provides protection in a relatively simple fashion, the sacrificial zinc dissolves over time, requiring regular replacement. In addition, this technique also does not provide observable feedback on how much protection is active. There are also environmental concerns with continuously dissolving zinc into ocean water [7].

Impressed-current cathodic protection (ICCP) is an alternative, non-sacrificial technique. This approach actively injects current into the electrolyte to make the metals cathodic and avoid oxidation. This can be done in open-loop fashion, in which a programmed amount of current is injected through an anode (typically made of platinum or metal oxides) into the electrolyte. In closed-loop fashion, an ICCP system determines the system’s level of protection by sensing the reference potential of the object being protected. The reference potential is measured as the voltage difference between a working electrode (e.g., the hull of a ship) and reference electrode made of a half-cell such as Ag/AgCl in a NaCl solution [8]. The potential of the reference electrode is considered 0 V by convention. Using a feedback controller, an ICCP system injects current through the anode to drive the electrolyte’s reference potential to a desired value [6], [9]. Unlike SACP, this system does not require constant maintenance by divers to replace anodes. Also, when using closed-loop control the system provides actionable information about the current state of protection with the reference electrode measurements. Closed-loop control with SACP is also possible [10], but not widely implemented.

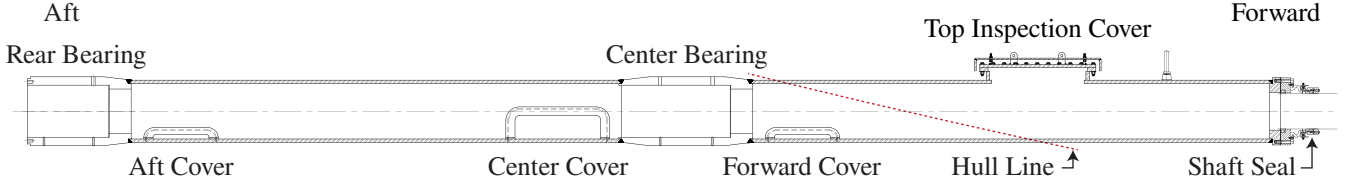


Fig. 1: Ship stern tube examined in this case study.

Modern ships commonly use a hybrid approach of both sacrificial anode and impressed current cathodic protection [3], [6], [11]. Some areas of the ship, e.g., bow thrusters or sea chests, are filled with seawater but partially enclosed. ICCP current may not protect these areas sufficiently. As a result, protecting these spaces requires sacrificial anodes. Unfortunately, these two techniques can interfere with each other. When sacrificial anodes are placed near reference electrodes for closed-loop ICCP, they can influence the reference potential measurements, causing the controller to mis-perceive the overall structure as protected based on a peak local reading. The system will then inject less current into the electrolyte, leaving more distant areas, farther from sacrificial anodes, to corrode. As an analogy, consider an HVAC system designed to heat a large room with closed-loop thermostatic control. Heat is injected into the room based on a controller's reading of the temperature at one particular location. If the temperature is still not to the occupants' preference, they may bring space heaters to warm localized parts of the room. Unfortunately, if a space heater is placed near the reference thermometer, the controller will perceive the room as well heated and inject less heat, to the discomfort of more distant occupants.

Installing both sacrificial and impressed current cathodic protection requires subtle analysis of a system's materials and geometry, especially in partially enclosed spaces. However, obtaining the necessary data for this analysis is difficult since the procedures must be carried out safely by divers. Previous research on corrosion measurement and cathodic protection planning relies heavily on numerical simulation [12]–[14]. These techniques are tremendously helpful for exploring design spaces. However, it is important to validate whether the realized system behaves as the simulation predicted. This requires instrumentation that can perform useful measurements in realistic conditions. This paper presents custom reference electrodes designed to leverage the existing geometry on a vessel experiencing corrosion. These are paired with a data acquisition system to capture reference potentials and impressed current around the ship. A circuit designed to dynamically adjust the behavior of an existing closed-loop ICCP system is presented. Using these instrumentation and measurement tools, techniques for system identification and protection status are developed.

II. CORROSION CASE STUDY

A vessel experiencing substantial galvanic corrosion serves as a case study for this work's field experiments. This vessel uses a hybrid cathodic protection system and has many partially enclosed spaces about the hull. The vessel's hull is made



Fig. 2: Severe ship stern tube corrosion in the form of pitting.

from A106B structural steel and is around 50 m in length. Two propellers with stainless steel shafts form the vessel's propulsion system. Each shaft is enclosed by a steel stern tube running from the ship's engine room to the propeller and is depicted in Fig. 1. The contour of the hull is also shown where the stern tube enters the ship's interior. Between the inner wall of the stern tube and the shaft is a clearance of approximately 5 cm. Water-lubricated polymer bearings support the shaft at the tube's aft end and middle. Four removable inspection covers provide access to the shaft: three on the underside of the tube adjacent to the bearings, and one on top of the tube at the forward end. Sacrificial zinc anodes mounted to the interior surface of each cover provide localized SACP. Each underside cover is secured with bolts and can be removed by divers. The stern tube is filled with seawater as the bearings and underside inspection covers are not watertight. The hull of the ship and both the interior and exterior surfaces of the stern tube employ a durable coating to prevent corrosion and reduce the load on cathodic protection measures. Some components, including the propeller shafts, propellers, and bow thruster do not have coatings.

During a routine dry dock period in which the propeller shafts were removed, inspectors found severe galvanic corrosion damage to the tube concentrated at areas close to the bearings. Fig. 2 shows deep pitting in the stern tube steel after sandblasting. This picture is taken from the opening for the aft inspection cover, facing the aft end of the tube. Note that the polymer bearing staves are shown in this picture but are not depicted in Fig. 1. When the shaft is inserted, seawater is able to pass through the small, longitudinal grooves in the bearing staves. The severe pitting required sections of the stern tube

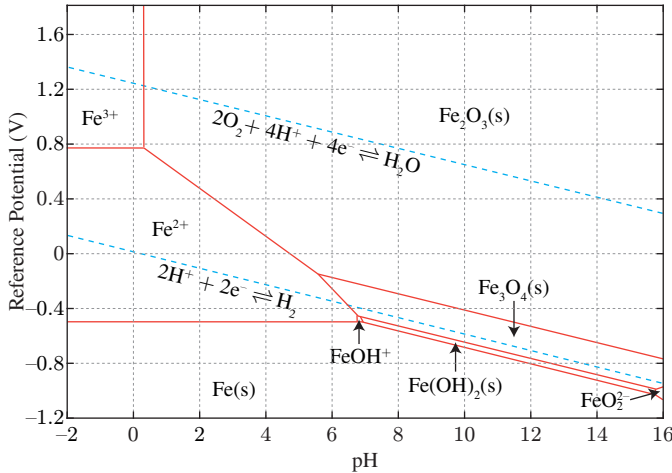


Fig. 3: Pourbaix diagram of iron adapted from [15]. Potential measured against the standard hydrogen electrode.

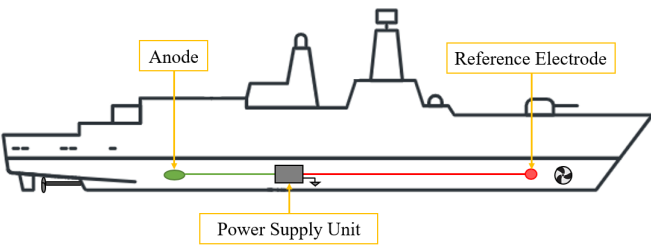


Fig. 4: Shipboard ICCP configuration.

to be replaced with new steel. In addition, the zinc anodes were nearly fully dissolved, despite not being used past their intended lifetime. As part of a root cause investigation into the unexpected corrosion, this section presents an examination of the ship's hybrid cathodic protection system.

A. Hybrid Cathodic Protection

Measuring the voltage of the structure to be protected with respect to a standardized half-cell in seawater indicates the level of corrosion protection. It is important to note that, consistent with the definition of *reference potential* in electrochemistry, this voltage measurement is made such that 0 V is defined to be the voltage of a particular reference electrode in the electrolyte (rather than the structure being protected). Injecting current into the water from the ship, which would increase the potential of the water relative to the hull, actually decreases the measurement of reference potential.

The Pourbaix diagram [3], [15] for iron (serving as a proxy for steel), given in Fig. 3, indicates the thermodynamically stable form of iron depending on pH and potential. This information indicates the reference potential required to prevent the oxidation reaction. For seawater with a pH around 8, the boundary of stability for Fe(s) is about -0.58 V relative to the standard hydrogen electrode. This is equivalent to -0.8 V relative to a Ag/AgCl reference electrode. This value is typically used as the maximum potential for the protection of steel in aerobic environments [3]. A reference potential lower (i.e. more negative) than this will keep solid iron stable.

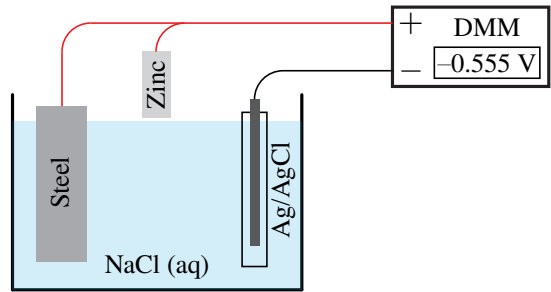


Fig. 5: Aquarium experiment with a steel plate and reference electrode in an electrolyte simulating the seawater. A digital multimeter (DMM) measures the potential between the steel and the reference electrode.

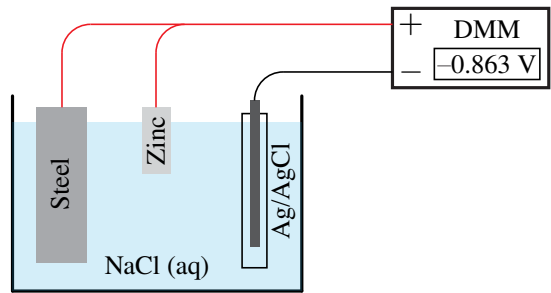


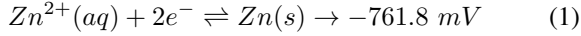
Fig. 6: Aquarium experiment with a steel plate, zinc anode, and reference electrode in an electrolyte simulating the seawater. A digital multimeter (DMM) measures the potential between the steel and the reference electrode.

However, water is not stable relative to hydrogen gas for any potential or pH at which Fe(s) is stable. As a result, creating a protective environment for iron forms hydrogen gas. As the reference potential is lowered, hydrogen gas forms at a higher rate, without providing additional protection for the steel. This phenomenon, known as overprotection, can cause unintended structural damage. Typically, reference potentials below -1.1 V are considered overprotective for this application [3], [16]. Steel alloys have varying degrees of susceptibility to hydrogen embrittlement [3], [4], [17] and can compromise the structural integrity of a hull over time. Overprotection can also cause cathodic disbondment of hull coatings [18]–[20], exposing more steel to seawater and increasing the dependence on cathodic protection measures.

The test vessel considered in this paper uses a combination of SACP and ICCP to protect its steel hull. The SACP takes the form of zinc anodes placed around the ship's exterior and inside the stern tube, bow thrusters, and other enclosed spaces. Fig. 4 illustrates the main components of the ICCP system and shows the approximate location of the components on the test ship. A central dc power supply injects current through both port and starboard anodes, located on the aft end of the ship. Two Ag/AgCl reference electrodes are mounted on the forward end of the ship, one on the port and one on the starboard side. The two reference electrodes are mounted in close proximity to the bow thruster tunnels, which contain a large number of zinc anodes.

The ICCP system is rated for a total maximum output current of 100 A, and two constant current power supplies inside the power supply unit ensure that the port and starboard anodes receive an equal current. The power supply adjusts the total output current in 0.1 A steps at a rate of 1 Hz, in a rate-limited fashion. By default, the target setpoint value for the electrodes is -0.85 V, and the feedback signal is created with the average of the two reference electrode readings. This setpoint ensures that the hull in close proximity to the reference electrodes is on the low end of the ideal protection range. If the average reference potential value is higher than the setpoint, the anode current will increase until the setpoint is reached. If the average reference potential value is lower than the setpoint, anode current will decrease. If the anode current reaches zero before the setpoint is reached, then the ICCP will effectively remain off and will lose the ability to drive the reference potential to the desired value.

Consider a case in which the ICCP is not injecting current. The reference potential is largely governed by the galvanic cell potential between the zinc and Ag/AgCl reference electrode. Based on the standard reduction potentials



and



this potential is around -984 mV, indicating sufficient protection around the Ag/AgCl reference electrode. However, this measurement provides little indication of the level of protection further away from the reference electrodes and in enclosed spaces. This is problematic, because these types of spaces may rely on ICCP current for sufficient protection.

To illustrate this point, consider the experiment shown in Figures 5 to 6. These tests were performed in a 10 gallon (37.9 L) aquarium filled to around 25% capacity with a 35 g/L solution of Instant Ocean sea salt, primary composed of NaCl. In the first case, a reference electrode is placed in the electrolyte along with a bare piece of steel similar to the hull steel of the test vessel. A voltmeter measures the potential between the steel and electrode. A piece of zinc is electrically connected to the steel, but is not in the electrolyte, making the path an open circuit. The reference potential measures -555 mV, which indicates severe underprotection. The measurement is repeated with the zinc lowered into the electrolyte. The reference potential measures -863 mV, slightly below the default target value for the test vessel's closed-loop ICCP system. If such an ICCP system were connected to this setup, it would inject no current, because the zinc provides a sufficiently protective potential in the region near the reference electrode.

The reference potential around the vessel is not an equipotential. Areas without a coating, either from damage, age, or lack of access when the ship is supported by blocks in dry dock, act as current sinks for cathodic protection current. ICCP and SACP systems both provide sources of current. Because all of this current flows through a moderately conductive medium, i.e., the seawater, there will be substantial potential gradients that are concentrated near current sinks or sources.

Day	Sea Temp (°F)	ICCP Current (A)	Anode Voltage (V)	Port Ref (mV)	Stbd Ref (mV)
1	68	1	2.2	-850	-850
2	72	1	2.2	-850	-850
3	64	0	0.9	-865	-870
4	64	0	0.9	-880	-880
5	68	0	1.8	-845	-855
6	60	0	1.0	-900	-900
7	60	0	1.0	-910	-910
8	69	1	2.1	-850	-850
9				(data not recorded)	
10	76	0	0.9	-875	-875
11	60	0	1.0	-930	-930
12	71	0	1.0	-910	-910
13	61	1	2.1	-855	-850
14	66	1	2.1	-850	-850
15	70	1	2.2	-850	-850
16	59	1	2.2	-850	-845

Fig. 7: Log sheet for an ICCP on a ship of the same class as the test ship.

In particular, the proximity of the reference electrodes to bow thruster zinc anodes can provide overly optimistic readings. Enclosed spaces, such as the stern tube will differ even more from the sensor readings as the highly restricted electrolyte conduction path will lead to large potential gradients between the inside and outside of the tube. This effect is difficult to observe in a lab setting, particularly since the vessel being considered is large.

B. Log Review

Standard operating procedure for the test vessel includes manual, daily recording of ICCP system parameters. Fig. 7 shows actual log sheet data, logging information about ICCP output current, average ICCP anode voltage, and the voltage of each reference electrode. Each day the reported ICCP current is either 0 or 1 A. On days with non-zero ICCP current, the average potential is -850 mV (± 2.5 mV). On days with zero current, average potentials are below -850 mV, as low as -930 mV. On these days, the sacrificial zinc anodes provide sufficient apparent protection and drive the reference potentials to the setpoint without any ICCP current. A minor exception is day five, in which the elevated anode voltage indicates current is flowing, but the limited resolution of the current readout is responsible for the current reading of zero. This log's data is consistent with the previous section's conclusion: the zines on the ship are sufficient to prevent the ICCP from injecting significant current. Due to the ship's configuration, ICCP current aids with protecting the rear of the ship where corrosion issues often occur. These corroded areas are likely underprotected due to the lack of ICCP current.

III. FIELD EXPERIMENT HARDWARE

Custom field equipment and instrumentation were developed to measure how effectively the internal zinc anodes and the ICCP system protect the stern tube (where corrosion was observed). Custom reference electrodes can probe the interior of the stern tube without changing its geometry. A "voltage adjuster" interfaces between the reference electrodes and the ICCP's power supply, enabling real-time changes to the ICCP's closed-loop setpoint. This field equipment enables



Fig. 8: Screw-type Ag/AgCl reference electrode.

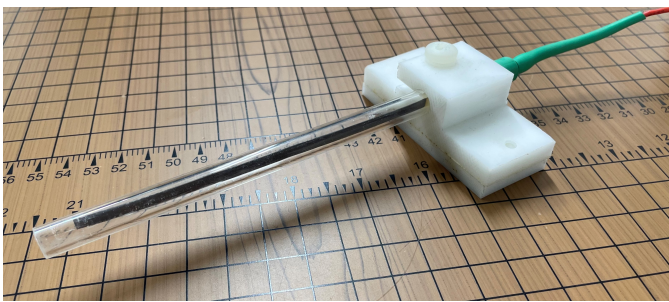


Fig. 9: Stick-type Ag/AgCl reference electrode.

an experiment to perturb the cathodic protection system and observe the resulting behavior.

A. Custom Reference Electrodes

Several practical constraints influence the design of the custom reference electrodes. The electrodes must securely remain in a consistent position across experimental setups. Since the ICCP system is unsafe to operate with divers in the water, the electrodes cannot be held by a diver. Because the stern tube's interior is of primary interest, the electrodes must be inserted into the tube without creating new gaps or openings in the tube. The tube also cannot be permanently modified by drilling holes. To satisfy these constraints, the custom reference electrodes were designed to penetrate the stern tube through the pre-existing screw holes in the inspection covers.

Each of the three lower inspection covers is secured with several 3/8-16 machine screws. The screws thread into a flange that is part of the tube, and the threaded holes extend all the way through into the interior of the tube. In addition, the corrosion was observed to be worst in close proximity to the bearing. The inspection covers are adjacent to the bearings, providing the ideal opportunity to take worst-case measurements. The threaded holes are too small for a commercial electrode and require custom instrumentation.

Fig. 8 shows the custom “screw-type” reference electrode. This electrode is manufactured by first screwing a 3/8-16 threaded nylon rod into a chamfered cylinder that makes up the rear of the electrode. The chamfer on the cylinder

mimics the design of the screw, ensuring it seals the hole as much as the original countersunk screw. A hole is drilled through the side of the cylinder and a nylon rod is inserted to make a handle. The pieces are epoxied together and an axial hole is drilled all the way through the threaded rod. After soldering a strip of high purity silver to a cable, the silver is inserted into the screw and epoxied in place. The epoxy mechanically secures the silver and wire in place and electrically isolates the solder joint and copper wire. Exposing these other metals to the seawater would form a galvanic cell and cause incorrect readings. A vent hole is drilled in the side of the threaded rod to allow air to escape when submerging the electrode. This vent hole is sufficiently close to the end of the screw that it remains past the threaded flange when installed. Finally, the surface of the silver is converted to silver chloride upon immersion in a solution of ferric chloride for about 48 hours [21]. Formation of AgCl by chloridization of the silver in 0.1 M HCl was also used with very similar results [8]. The cable is terminated with a waterproof barrel jack connector to allow long cabling to be easily connected to the electrode after installation. These reference electrodes are constructed differently from typical laboratory reference electrodes. However, the design of the electrodes is intended to mimic that of the permanently installed ship electrodes to produce better agreement.

Large currents in the partially conductive seawater create large gradients in the electrolyte potential [9], [22]–[24]. Since the experiments to be performed may result in large ICCP currents, the potential in the area surrounding the ICCP anodes should be monitored. These anodes are surrounded with a dielectric shield that can withstand overprotection without being damaged. Two additional electrodes are designed to monitor the potential fore and aft of the ICCP anode. Fig. 9 shows an example of these “stick-type” electrodes made from acrylic tubes. A strip of silver is soldered to wire and epoxied in place. The surface of the silver is converted to AgCl in the same manner as the screw-type electrodes. A holder made with Delrin and neodymium magnets allows this electrode to be attached anywhere on the steel hull.

B. Voltage Adjuster

Fig. 10 shows the voltage adjuster used for these experiments. The adjuster is based on a PSoC 5LP system-on-chip development board. Potentiometers, buttons, and an LCD screen provide a simple interface to let the operator offset the reference electrode signals passing through the adjuster. Fig. 11 shows the feedback loop of the ICCP with the adjuster installed in the loop. For simplicity, only one reference electrode is considered as the ICCP uses the average of the two reference electrode voltages for feedback purposes. To perform *in situ* reference voltage adjustment, the test vessel's reference electrode wires are disconnected from the ICCP power supply and instead connected to the voltage adjuster (as shown in the right side of Fig. 11). The voltages are buffered and then sampled by the microcontroller's internal successive approximation register (SAR) analog-to-digital converter (ADC). Each reference voltage signal is digitally shifted by a user-chosen

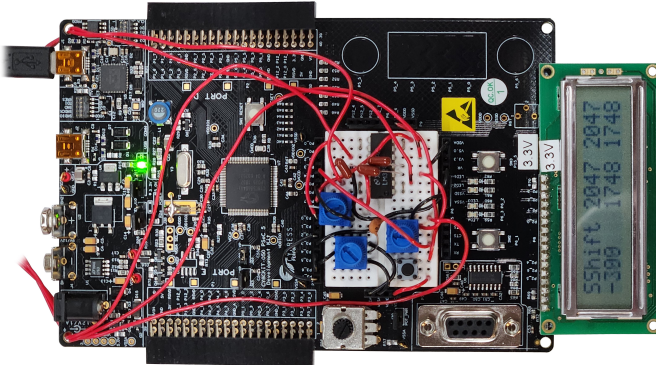


Fig. 10: System-on-chip reference voltage adjuster provides a single-IC solution (shown here on a development board) to modify installed ICCP behavior.

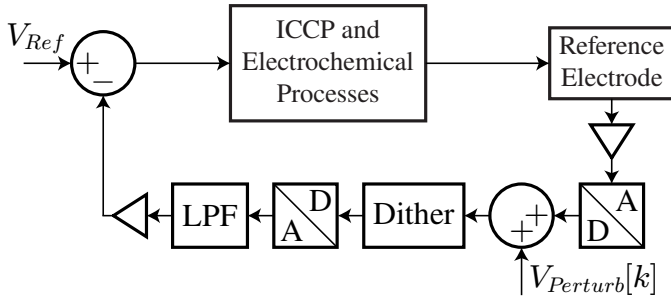


Fig. 11: ICCP reference voltage adjuster circuit.

value before being passed to the digital-to-analog converter (DAC). The 8-bit DAC is extended by four bits with dithering to improve resolution. The output is passed through a low-pass filter (LPF) and a buffer, and then finally wired back into the ICCP system. By introducing this digital voltage shift, the target reference voltage can be modified dynamically. The new target voltage follows

$$V_{ref,new}(t) = V_{ref} - V_{Perturb}(t) \quad (3)$$

and thus the ICCP controller effectively takes the form given in Fig. 12. As implied by the new control loop, the voltage adjuster does not significantly affect the dynamics of the ICCP feedback loop, and merely serves as a means to adjust the reference signal. The perturbation voltage $V_{Perturb}(t)$ can take an arbitrary form, such as a constant offset or an oscillating perturbation. That is, the adjuster can be used to effectively move an ICCP setpoint that cannot otherwise be changed. The adjuster can also conduct dynamic experiments that vary ICCP current, providing richer signals for state and parameter estimation.

IV. FIELD EXPERIMENTS

Using the specialized measurement equipment, an experiment on the test vessel empirically determines the effectiveness of the hybrid cathodic protection scheme inside the stern tube. This experiment is performed over a range of zinc anode conditions, meant to approximate the zincs' lifespans.

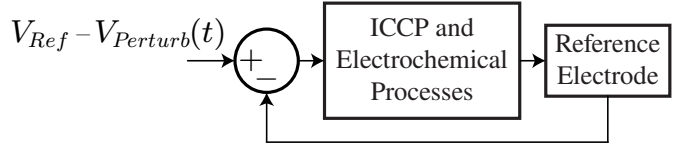


Fig. 12: ICCP control loop approximation with voltage adjuster.



Fig. 13: Screw-type electrode installed in the stern tube inspection cover.

In total, there are 10 different useful quantities that need to be monitored for the following experiments, given as follows:

- 3 screw-type electrode voltages (in stern tube interior)
- 2 stick-type electrode voltages (near ICCP anode)
- 2 built-in reference electrode voltages
- Total ICCP output current
- Shaft voltage
- Shaft-to-hull current

A ten-channel Hioki data logger with a maximum sample rate of 20 Hz per channel records these ten values. The following series of tests are performed during routine ship maintenance, in which all of the test vessel's zinc anodes are replaced by a team of divers.

A. Procedure

The experiment to determine the effectiveness of the cathodic protection system is split into three parts. The equipment was set up, including the insertion of the screw electrodes and attachment of the stick electrodes. The three screw electrodes were used to replace one screw in each of the lower stern tube inspection covers. Fig. 13. shows a screw electrode inserted on the aft side of the forward inspection cover. The camera faces forward and up, and the stern tube hull penetration is visible. The electrodes were placed in one of the holes that is closest to the bearing. The stick electrodes were attached to the hull just fore and aft of one of the ICCP anodes, and at the edge of the dielectric shield. All five sensor

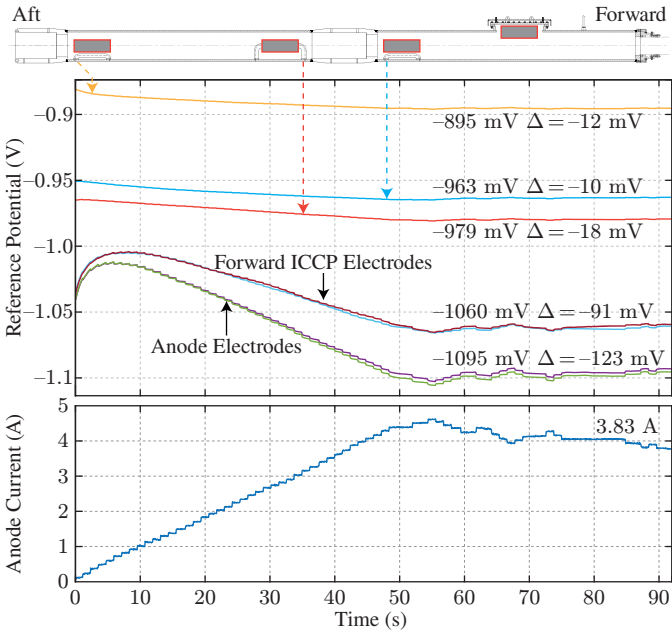


Fig. 14: ICCP target modification with old zinc anodes.



Fig. 15: Heavily depleted area zinc anode after one year.

wires were routed back into the engine room and connected to the data logger. The voltage adjuster was inserted between the electrodes and the ICCP system, and the voltage inputs to the adjuster were also fed into the data logger. Hall-effect DC current probes were attached to the ICCP ground return wire and the shaft brush ground wire. The shaft voltage was monitored with a direct ohmic connection to the shaft.

The following tests were completed:

- 1) Static measurements with the ICCP target artificially set to values as low as -1200 mV
- 2) Dynamic measurements with ac injections from 10 mHz to 10 Hz
- 3) Open loop ICCP current control steps up to 30 A

After the first set of tests was complete, divers entered the water to replace the zinc anodes on the vessel. The zinc anodes mounted to the inside of the inspection covers on the stern tube being tested were removed rather than replaced. As a result, the only zinc left inside the tube was mounted to the top-side inspection cover, which can only be removed in dry

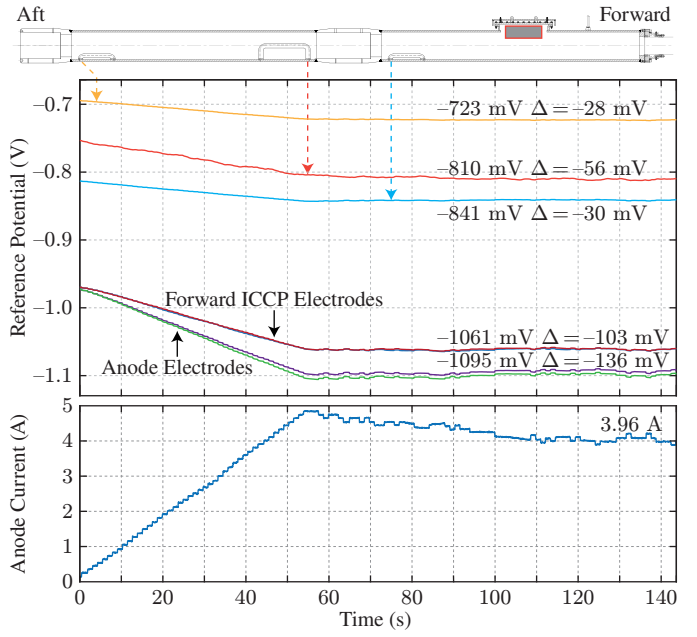


Fig. 16: ICCP target modification with no zinc anodes.

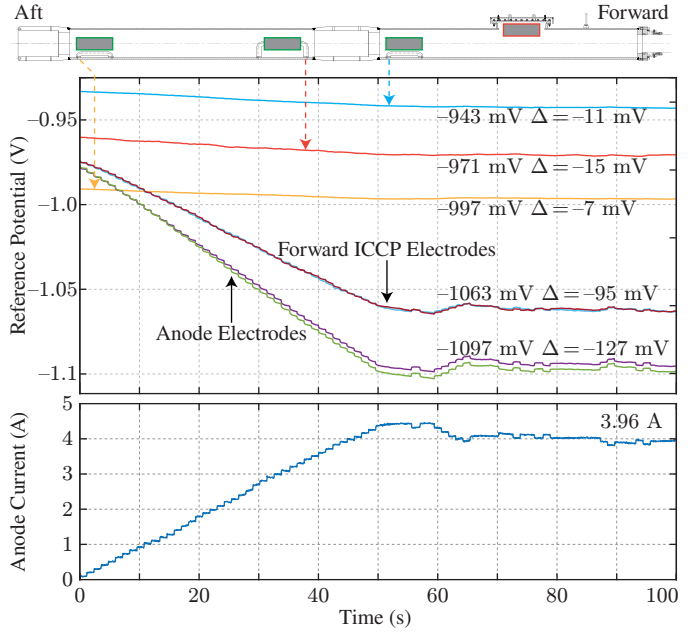


Fig. 17: ICCP target modification with new zinc anodes.

dock. Accordingly, the forward compartment of the stern tube still had zinc protection, but the aft compartment did not. The inspection covers were replaced and the screw electrodes reattached and the tests were repeated. Finally, the divers installed new zinc anodes on the inside of each inspection cover and the tests were completed a third time.

B. Static Analysis (Closed Loop)

Fig. 14 shows a setpoint adjustment test for the first configuration, in which the old zincs were present in the stern tube. These old anodes were in use for approximately

one year at the time of the test. The ICCP setpoint was changed from -850 mV to -1050 mV using the voltage adjuster, and the ICCP current adjusts accordingly. The graph is annotated with steady-state values, and the deviation between the measurement before and after the setpoint adjustment. The anode current increases in a stair-step pattern due to the action of the controller. Eventually, the system enters steady state with the ICCP electrodes reading close to the setpoint. As the current increases, the difference between the ICCP electrodes' and the stick electrodes' voltages increases approximately linearly. The deviation is indicative of the moderately conductive medium that the ICCP current passes through. This shows experimental evidence of the placement of reference electrodes affecting the measurement. A reading taken at only one part of the ship does not provide a complete picture about the level of protection around the ship. The three screw electrode potential readings are shown in yellow, blue, and red, along with their physical positions along the stern tube. Each electrode indicates some level of improvement in protection, indicating that ICCP current is successfully entering the enclosed space. In each case, the initial values shows a high level of protection. The stern tube drawing also indicates the condition and position of zinc anodes as outlined, gray rectangles. The red outline indicates a degraded anode, while green refers to a new anode. The rectangles are not to scale and also do not show the relative size of different anodes in the stern tube.

In this configuration, the zinc anodes are heavily depleted but not entirely gone. Fig. 15 shows the depleted zinc anodes removed from the inspection covers of both stern tubes. About 80% of the original zinc mass is gone in the zinc anodes shown. Most of this remaining zinc is coated in biological fouling, decreasing the effective surface area. This test shows that the old zinc anodes are providing sufficient protection regardless of ICCP current for this configuration. However, the readings will be substantially different when the shaft rotates. The mixing of the electrolyte inside the tube will substantially increase the current demanded from the zinc anodes [25], [26]. The stainless steel shaft in the biologically active seawater environment will form a passivating film when the water surface velocity is low. When propelling the ship however, this film is removed and the large surface area of the bare-metal shaft demands a large amount of cathodic protection current. The electrolyte potential the zinc anodes can maintain will not provide as much protection in this situation, and the anodes will deteriorate rapidly.

Fig. 16 shows the results of these tests for the second configuration. During this test, the exterior zinc anodes were replaced with new ones and the three removable inspection covers' zincs were removed without being replaced. Interestingly, the ICCP reference electrode and current readings are largely the same as in the previous test. The custom screw electrodes tell a far different story, however, showing marginal protection at best when the ICCP is off. The deviations between measurements before and after the setpoint change increase significantly as the greater potential difference across the wall of the stern tube allows more current to enter. This test may be a better indicator of how aged zincs perform when

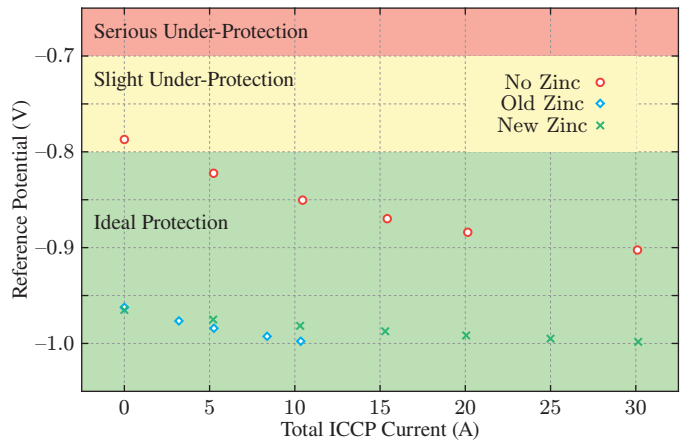


Fig. 18: Forward inspection cover electrode readings vs. ICCP current for all three zinc conditions.

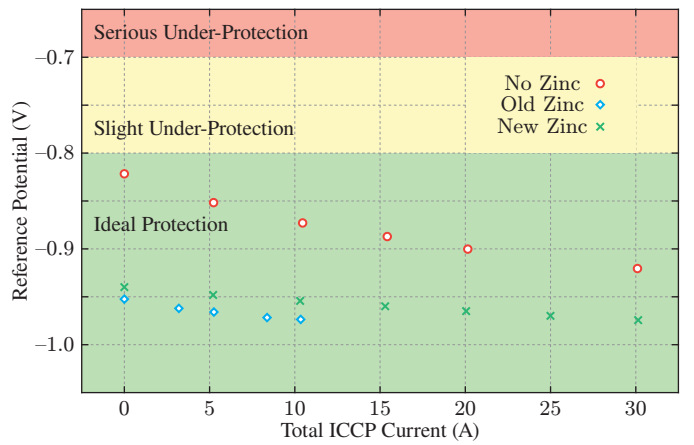


Fig. 19: Center inspection cover electrode readings vs. ICCP current for all three zinc conditions.

under heavy cathodic load, such as when the shaft rotates. The change in ICCP setpoint appears to provide additional protection inside the stern tube without pushing the outside of the ship into overprotection. The screw electrodes also show that there is more protection toward the fore end of the tube than the aft, potentially due to the large zinc plate inside of the top inspection cover.

Fig. 17 shows the test results for the final configuration, in which new zincks were installed in the three removable inspection covers. The ICCP's external electrodes report similar readings as before. The initial reference potential values are somewhat larger, but this can result from various environmental factors such as interference from other nearby cathodic protection systems, salinity, and temperature. With new zinc anodes, all three screw electrodes report adequate protection.

The ICCP setpoint adjustment results in very small changes in screw electrode readings, which is consistent with the new zincks sourcing more current than the old degraded zincks. Even without a significant improvement in reference potential, the ICCP current still benefits the stern tube because it decreases the surface current required of the zinc anodes, extending their lifespans.

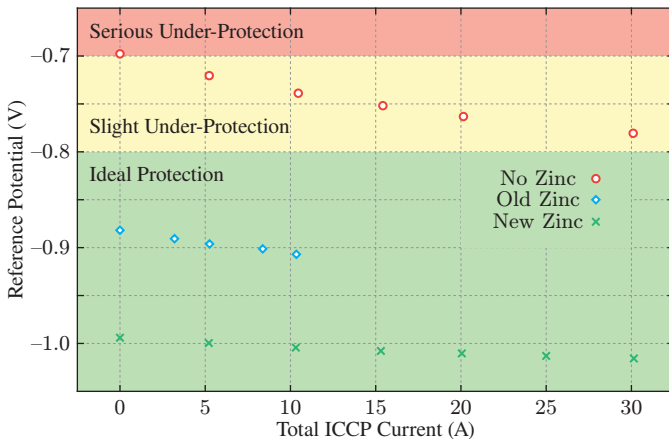


Fig. 20: Aft inspection cover electrode readings vs. ICCP current for all three zinc conditions.

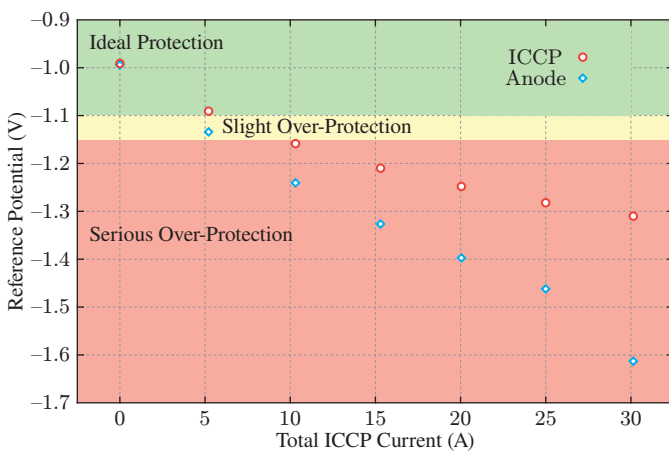


Fig. 21: Exterior reference electrodes readings vs. ICCP current.

C. Static Analysis (Open Loop)

The previous tests involved relatively minor changes to the ICCP setpoint in closed loop. A set of open loop current control tests was performed to determine how higher current levels affect the protection of the stern tube and ship exterior. Figures 18 to 20 show the reference electrode values inside the stern tube for the forward, middle, and aft inspection covers respectively. These tests used a range of current values between 0 A and 30 A. These plots indicate that increasing the ICCP current significantly improves the level of protection inside the stern tube, particularly in the “No Zinc” case. In some cases, the old zinc anodes provide better protection than the new ones. New zinc anodes are often contaminated with oils from handling and storage, decreasing their effective surface area. The aft cover is a particularly difficult location to protect, as is apparent in the slight underprotection at 30 A of ICCP current (30% of its capacity).

Figures 19 and 20 show the results for the center and forward screw electrode values. While the results from the center cover are similar to those with the forward cover, the aft results show a more dramatic dependence on zinc condition. The old zinc cannot achieve the same level of protection

as in other locations, and could be the result of a greater demand for protection current from exposed metal surfaces, or more advance zinc degradation. The results without zinc are substantially worse at the aft cover, implying that this region experiences more current demand, which depletes its anodes at an accelerated rate. Recalling from Fig. 1 that the aft and center covers are in the same compartment, it is also interesting to note the large potential gradient inside the stern tube based on these test results.

At each location, the measured potential indicates that ICCP current is not necessary to achieve ideal protection as long as the zincons are not completely expended. However, protection current drawn by the shaft depends on its rotational speed, with a stationary shaft drawing the lowest amount of current. Further, marginal changes in reference potential have substantial impact on the life of zinc anodes and this effect will be explored in Section V.

The exterior ICCP electrodes provide indications of overprotection when the ICCP outputs high current, as shown in Fig. 21. These results were captured after new zincons were installed. As expected, the stick electrodes placed very close to one of the anodes experienced reduced potentials relative to the ICCP electrodes because the seawater acts as a poor conductor. As is typical of conductive media, there is a large gradient in reference potential near point sources of current such as the ICCP anodes. Even with only 5 A of ICCP current, the anode electrodes show some amount of overprotection. A dielectric shield is used near the anodes to reinforce the hull coating to prevent cathodic disbondment, but the electrodes are close to the edge of this shield. Higher currents, such as in the 30 A test, show that the ICCP current cannot be set arbitrarily high in order to protect the shaft tube as the entire exterior of the ship will be at the risk of cathodic disbondment.

D. Dynamic Analysis

Electrochemical systems have time constants just like any electrical system. These time constants may depend on system factors such as the exposed zinc surface area in the stern tube. The screw electrodes cannot be used when the ship is underway as the wires are likely to become tangled in the propellers. However, the propeller shaft is a large, uncoated object inside the stern tube that participates in the electrochemical reaction. By injecting known frequencies into the ICCP current and monitoring the shaft voltage, an empirical transfer function estimate (ETFE) [27]–[30] can be constructed as shown in (4).

$$H(\omega) = \frac{V(\omega)}{I(\omega)} = \frac{\sum_{n=0}^{N-1} v_{\text{shaft}}[n]e^{-j\omega t_n}}{\sum_{n=0}^{N-1} i_{\text{iccp}}[n]e^{-j\omega t_n}} \quad (4)$$

Direct measurement of zinc status is possible [31], but the ETFE may assist in identifying zinc condition inside the stern tube in a nonintrusive fashion. This analysis could be further improved with remote monitors [23], [32]–[35] that can measure internal stern tube potential while underway.

The voltage adjuster can create currents at known frequencies by offsetting the reference electrode potentials by a chosen sinusoidal value. This sinusoidal offset frequency was varied between 10 mHz and 10 Hz (half the sampling rate of the

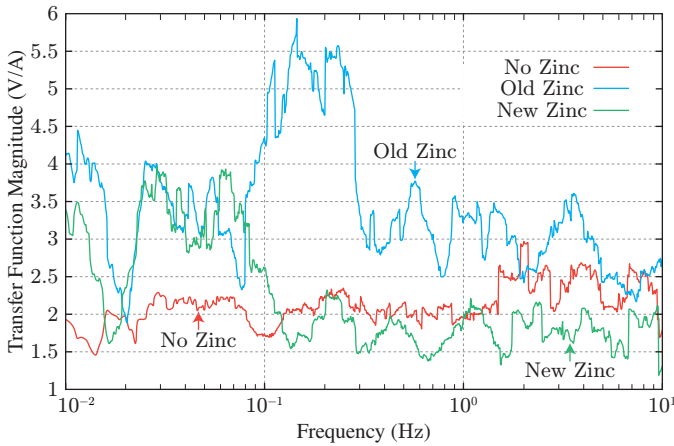


Fig. 22: ETFE results between ICCP current and shaft voltage for the different zinc conditions.

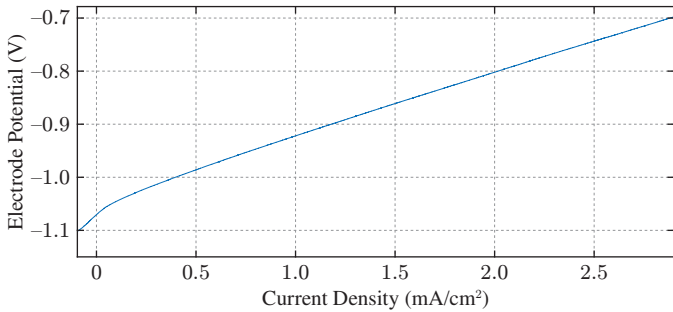


Fig. 23: Electrode potential vs. current density for zinc in a 35 g/L NaCl solution.

data logger). The rate-limited ICCP controller substantially limits the range of injected current frequencies. The ETFE is shown in Fig. 22 for the three different zinc conditions. Each ETFE result is smoothed with an adaptive Hamming window with frequency width proportional to the frequency of interest. Each zinc configuration has a distinct ETFE characteristic, suggesting that a data-driven model could determine zinc life from a nonintrusive set of measurements. The frequency extent of the ETFE result is limited by the experimental setup, and there may be more interesting behavior at higher frequencies. However, due to the specialized current injection equipment required, this must be explored more in future work.

V. SACRIFICIAL ANODES LIFETIME ESTIMATION

As the reference potential rises, sacrificial zinc anodes become more heavily loaded and inject more current into the electrolyte. This current density relationship is shown in a polarization curve [3], [11], [15], [36]. A polarization curve for this system was generated in the lab using zinc alloy and seawater gathered from Boston Harbor. The resulting curve is shown in Figures 23 to 24 with linear and logarithmic current density scales, respectively. Note that the curve with logarithmic current includes both positive and negative current data, causing the reversal on the left side of the curve. Whereas Ohm's law can provide information about current based on a measured voltage, the polarization curve provides

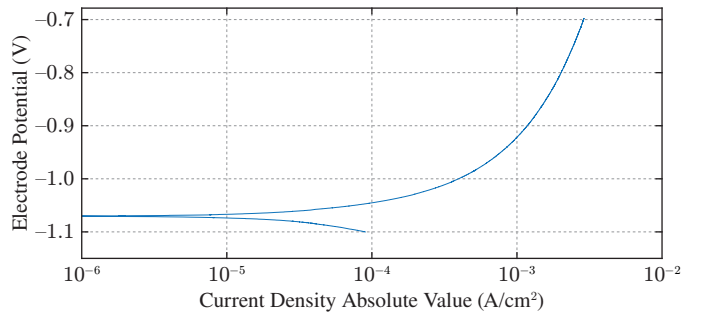


Fig. 24: Electrode potential vs. log current density for zinc in a 35 g/L NaCl solution.

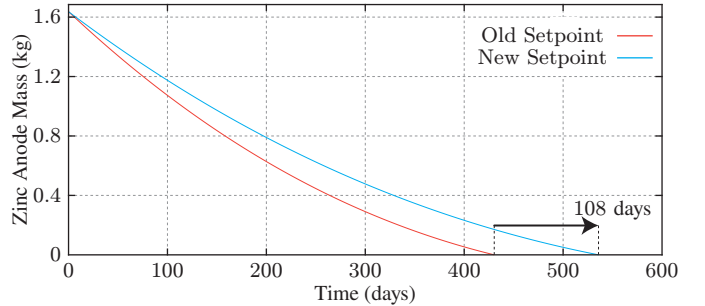


Fig. 25: Center inspection cover estimated zinc lifespan for the original and modified ICCP setpoint.

the current density from a measured potential. Therefore, the screw electrode measurements enable estimation of the rate at which stern tube zinc anodes are consumed, permitting a calculation of expected lifetime.

The zinc anodes mounted to the inside of the inspection covers measure approximately 1x2x7 inches (about 2.54x5.08x17.78 cm). If the reference potential can be reasonably assumed to be constant over time, then the surface current will also be constant based on the polarization curve. The zinc will dissolve at a rate of

$$R_{Zn} = \frac{J_n A(t)}{\rho_c \eta} \quad (5)$$

where J_n is the current density from the polarization curve normal to the surface, $A(t)$ is the surface area as a function of time, ρ_c is the specific charge density and indicates how much charge is needed to dissolve the anode per unit mass, and η is the charge efficiency. Anodes experience some self corrosion, and with a typical factor of $\eta = 0.95$, $\rho_c \eta = 779$ Ah/kg [37].

A simulation of zinc mass loss over time is performed assuming a uniform surface current density, no coatings or films, constant reference potential over time, and a 95% charge efficiency for the sacrificial anode (779 Ah/kg). R_{Zn} divided by the density of the material and $A(t)$ yields the rate at which all surfaces recede in depth. This is used to determine how the dimensions change with time and $A(t)$ is updated accordingly. Fig. 25 shows the resulting zinc mass over time. The mass decreases more slowly with time as less zinc surface area is exposed to the electrolyte. The reference potentials in this study are from the center inspection cover screw electrode

when the ICCP setpoint was either -850 mV or -1050 mV, with old zinc anodes. Although the adjusted setpoint only decreased the reference potential by 18 mV, the expected lifetime of the zinc anodes increased from 426.5 to 534.4 days (a 25.3% increase). This zinc lifespan estimation technique enables a better informed analysis of the tradeoff between increased ICCP setpoint and zinc lifespan.

VI. CONCLUSION

Corrosion prevention is critical to maintaining high-value assets whenever seawater is present. Prevention techniques are often not informed by *in situ* measurements. Accordingly, they do not seek to optimize the performance and longevity of the cathodic protection system. The custom instrumentation and interface equipment presented in this work simultaneously measures the performance of a hybrid cathodic protection system in various locations across different conditions. In particular, the screw electrodes enable measurement of a difficult-to-protect, partially enclosed space without significantly affecting the system geometry. The resulting data enables ICCP setpoint optimization for more effective cathodic protection. Nonintrusive methods enabled by the ETFE allow lifespan estimation of sacrificial anodes in spaces difficult to monitor outside of scheduled maintenance periods.

REFERENCES

- [1] H.-J. Chung, C.-S. Yang, G.-W. Jeung, J.-J. Jeon, and D.-H. Kim, "Accurate prediction of unknown corrosion currents distributed on the hull of a naval ship utilizing material sensitivity analysis," *IEEE Transactions on Magnetics*, vol. 47, no. 5, pp. 1282–1285, 2011.
- [2] *CRC handbook of chemistry and physics*. Cleveland, Ohio: CRC Press, 1978.
- [3] C. G. Googan, *Marine corrosion and cathodic protection*, 1st ed. Abingdon, Oxon: CRC Press, 2022.
- [4] A. Bahadori, *Cathodic corrosion protection systems: a guide for oil and gas industries*, 1st ed. Boston: Gulf Professional Publishing, 2014.
- [5] K. Altaf, M. Parvez, and M. Tanweer, "Part-i: Optimum designing of cathodic protection systems of marine platforms," in *2018 15th International Bhurban Conference on Applied Sciences and Technology (IBCAST)*, 2018, pp. 682–686.
- [6] D. E. Diedericks, G. van Schoor, and E. O. Ranft, "Cathodic protection system design framework," in *2019 Southern African Universities Power Engineering Conference/Robotics and Mechatronics/Pattern Recognition Association of South Africa (SAUPEC/RobMech/PRASA)*, 2019, pp. 530–537.
- [7] C. Rousseau, F. Baraud, L. Leleyter, and G. O., "Cathodic protection by zinc sacrificial anodes: impact on marine sediment metallic contamination," *Journal of hazardous materials*, vol. 167, no. 1-3, pp. 953–958, 2009.
- [8] C. G. Zoski, *Handbook of electrochemistry*, 1st ed. Amsterdam: Elsevier, 2007.
- [9] L. Mrdović and Š. Ivošević, "Applications impressed current cathodic protection of the ship hull," in *2023 27th International Conference on Information Technology (IT)*, 2023, pp. 1–4.
- [10] F. Ferraris, M. Parvis, E. Angelini, and S. Grassini, "Measuring system for enhanced cathodic corrosion protection," in *2012 IEEE International Instrumentation and Measurement Technology Conference Proceedings*, 2012, pp. 1583–1587.
- [11] C. Thiel, K. Neumann, C. Broeckeler, M. Jalali, F. Ludwar, A. Rennings, J. Doose, and D. Erni, "Iterative electric potential adjustment of damaged naval vessels using the onboard iccp system," in *2018 COMSOL Conference in Lausanne*, 2018, pp. 1–6.
- [12] D. T. Kalovelonis, D. C. Rodopoulos, T. V. Gortsas, D. Polyzos, and S. V. Tsipopoulos, "Cathodic protection of a container ship using a detailed bem model," *Journal of Marine Science and Engineering*, vol. 8, no. 5, 2020.
- [13] E. Santana-Diaz and R. Adey, "Predicting the coating condition on ships using iccp system data," *International Journal for Numerical Methods in Engineering*, vol. 62, no. 6, pp. 727–746, 2005.
- [14] S. Xing, Y. Li, H. Song, Y. Yan, and M. Sun, "Optimization the quantity, locations and output currents of anodes to improve cathodic protection effect of semi-submersible crane vessel," *Ocean Engineering*, vol. 113, pp. 144–150, 2016.
- [15] Wikibooks, "Introduction to Inorganic Chemistry," 2024, [Online; accessed 23-April-2024].
- [16] "En 16222:2012 cathodic protection of ship hulls," Association Française de Normalisation, La Plaine Saint-Denis, France, Standard, Dec. 2012.
- [17] H. K. D. H. Bhadeshia and H. K. D. H. Bhadeshia, "Prevention of hydrogen embrittlement in steels," *ISIJ international*, vol. 56, no. 1, pp. 24–36, 2016.
- [18] T. S. Ramotowski, W. C. Tucker, and M. A. Rice, "Cathodic debonding of undersea electronic cable connectors: Delamination kinetics when primers and encapsulants are bonded directly to bare metal connector backshells," in *2013 OCEANS - San Diego*, 2013, pp. 1–6.
- [19] T. S. Ramotowski, A. M. Duszkiewicz, and M. A. Rice, "Design considerations for accelerated life tests conducted on cable hardware subject to cathodic delamination," in *OCEANS 2016 MTS/IEEE Monterey*, 2016, pp. 1–6.
- [20] T. S. Ramotowski and M. Oyedepo, "The effect of environmental factors on the rate of cathodic delamination," in *OCEANS 2021: San Diego – Porto*, 2021, pp. 1–9.
- [21] D. Resnik, B. Pečar, M. Možek, N. Lokar, and D. Vrtačnik, "Formation of thin film Ag/AgCl reference electrode by electrochemical and chemical method," in *2019 42nd International Convention on Information and Communication Technology, Electronics and Microelectronics (MIPRO)*, 2019, pp. 41–46.
- [22] Q. Zhang, J. Lei, and L. Li, "Optimization of iccp anode configuration based on multi objective genetic algorithm," in *2019 International Conference on Computer Network, Electronic and Automation (ICCNEA)*, 2019, pp. 46–51.
- [23] P. Olszewski, A. Grabowski, M. Duncko, and S. Pedersen, "On cathodic protection monitoring and inspection of seabed pipelines," in *OCEANS 2023 - Limerick*, 2023, pp. 1–5.
- [24] P. Campbell, F. Kleiser, A. Weltin, J. Kieninger, S. J. Rupitsch, and U. G. Hofmann, "Electric field gradient sensing for offshore cathodic protection surveying," in *OCEANS 2023 - MTS/IEEE U.S. Gulf Coast*, 2023, pp. 1–6.
- [25] M. J. Bishop, "Preventing stern tube corrosion through shipboard cathodic protection," Master's thesis, Massachusetts Institute of Technology, June 2023.
- [26] I. C. Patnode, "Protecting our investment: Solving fast response cutter corrosion," Master's thesis, Massachusetts Institute of Technology, June 2023.
- [27] L. Ljung, *System Identification: Theory for the User*. Prentice-Hall, Inc., 1999.
- [28] E. K. Saathoff, S. R. Shaw, and S. B. Leeb, "Line impedance estimation," *IEEE Transactions on Instrumentation and Measurement*, vol. 70, pp. 1–10, 2021.
- [29] P. M. T. Broersen, "A comparison of transfer function estimators," *IEEE Transactions on Instrumentation and Measurement*, vol. 44, no. 3, pp. 657–661, 1995.
- [30] D. D. S. Mota, "Estimating the frequency response of an excitation system and synchronous generator: Sinusoidal disturbances versus empirical transfer function estimate," *IEEE Power and Energy Technology Systems Journal*, vol. 5, no. 2, pp. 27–34, 2018.
- [31] D. Tamhane, J. Thalapil, S. Banerjee, and S. Tallur, "Smart cathodic protection system for real-time quantitative assessment of corrosion of sacrificial anode based on electro-mechanical impedance (emi)," *IEEE Access*, vol. 9, pp. 12230–12240, 2021.
- [32] F. Abate, D. Di Caro, G. Di Leo, and A. Pietrosanto, "Towards a distributed monitoring system for gas pipeline cathodic protection," in *2018 IEEE International Instrumentation and Measurement Technology Conference (I2MTC)*, 2018, pp. 1–6.
- [33] A. Kara, M. A. Al Imran, and K. Karadag, "Linear wireless sensor networks for cathodic protection monitoring of pipelines," in *2019 International Conference on Mechatronics, Robotics and Systems Engineering (MoRSE)*, 2019, pp. 233–236.
- [34] M. Wongkhan, J. Thitasino, and P. Chaitragul, "Cathodic protection remote monitoring via lorawan technology of water pipelines," in *2023 3rd International Conference on Electrical, Computer, Communications and Mechatronics Engineering (ICECCME)*, 2023, pp. 1–6.

- [35] L. Ting and Z. Xiang, "Optimization of remote monitoring of cathodic protection power supply system base on four-tier structure and b/s model," in *2011 6th International Conference on Computer Science & Education (ICCSE)*, 2011, pp. 1346–1350.
- [36] A. Andre Chang, J. N. Patel, H. Shahbazbegian, and B. Kaminska, "An electro-chemical test and optimization system for impressed current cathodic corrosion protection," in *19th Annual International Mixed-Signals, Sensors, and Systems Test Workshop Proceedings*, 2014, pp. 1–5.
- [37] R. Sarfi, M. Salama, C. Gebotys, and A. Chikhani, "Optimal design of cathodic protection schemes: a power engineering applications," in *Proceedings of Canadian Conference on Electrical and Computer Engineering*, 1993, pp. 664–667 vol.2.



Erik K. Saathoff received the B.S. degree in electrical engineering from the University of Illinois at Urbana-Champaign in 2018, and the M.S., E.E., and Ph.D. degrees in electrical engineering and computer science from the Massachusetts Institute of Technology in 2021, 2023, and 2024, respectively. His research interests include high-performance power electronics, switched-capacitor converters, and system identification.



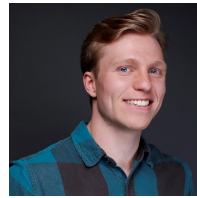
Michael J. Bishop received the B.S. degree in mechanical engineering from the U.S. Coast Guard Academy in 2019 and the M.S. degree in mechanical engineering from the Massachusetts Institute of Technology in 2023. He has served as a Deck Watch Officer and an Operations Officer of USCGC NATHAN BRUCKENTHAL (WPC 1128). He is a Lieutenant with the United States Coast Guard.



Isabelle C. Levitsky received the B.S. degree in naval architecture and marine engineering from the U.S. Coast Guard Academy in 2016 and the M.S. degree in mechanical engineering from the Massachusetts Institute of Technology in 2023. She has served on board USCGC ESCANABA (WMEC 907), as a port engineer for the IBCT product line, and as an engineering instructor at the U.S. Coast Guard Academy. She is a Lieutenant with the United States Coast Guard.



Jacob D. Skimmons is a staff engineer at the Coast Guard Marine Safety Center in Washington, DC. Previously he served as the damage control assistant on USCGC POLAR STAR (WAGB 10). He received a Bachelor of Science degree from the US Coast Guard Academy in 2020 and a Master of Science in Naval Architecture and Marine Engineering from the Massachusetts Institute of Technology in 2024. He is a Lieutenant with the United States Coast Guard.



energy systems.

Aaron W. Langham received the B.E.E. degree in electrical engineering from Auburn University, Auburn, AL, USA in 2018, and the M.S. and E.E. degrees in electrical engineering and computer science from the Massachusetts Institute of Technology, Cambridge, MA, USA in 2022 and 2024, respectively. He is currently pursuing the Ph.D. degree in electrical engineering and computer science at the Massachusetts Institute of Technology, Cambridge, MA, USA. His research interests include signal processing, machine learning, and IoT platforms for



Steven B. Leeb received the Ph.D. degree from the Massachusetts Institute of Technology, in 1993. Since 1993, he has been a member on the MIT Faculty with the Department of Electrical Engineering and Computer Science. He also holds a joint appointment with the Department of Mechanical Engineering, MIT. He is concerned with the development of signal processing algorithms for energy and real-time control applications.